Journal of Structural Geology 31 (2009) 960–971

Contents lists available at ScienceDirect

Journal of Structural Geology

journal homepage: www.elsevier.com/locate/jsg

The effect of fluid composition on the behavior of well cemented, quartz-rich sandstone during faulting

Charles M. Onasch [a,*], William M. Dunne [b], Jennie E. Cook [b], Allyson O'Kane [a]

[a] Department of Geology, Bowling Green State University, Bowling Green, OH 43403, USA
[b] Department of Earth and Planetary Sciences, University of Tennessee, Knoxville, TN 37996, USA

ARTICLE INFO

Article history:
Received 24 April 2007
Received in revised form
23 July 2008
Accepted 16 October 2008
Available online 6 November 2008

Keywords:
Faults
Fluids
Microstructures
Quartz arenite
Appalachians

ABSTRACT

Previous studies [O'Kane, A., Onasch, C.M., Farver, J., 2007. The role of fluids in low-temperature, fault-related deformation of quartz arenite. Journal of Structural Geology 29, 819–836; Cook, J., Dunne, W.M., Onasch, C.M., 2006. Development of a dilatant damage zone along a thrust relay in a low-porosity quartz arenite, Journal of Structural Geology 28, 776–792] found that quartz arenite within two fault zones in the Appalachian foreland thrust belt displays very different structural styles and histories despite deforming at similar pressures and temperatures during the Alleghanian orogeny. A comparison of the grain-scale deformation and fluid histories using transmitted and cathodoluminescence microscopy and fluid inclusion microthermometry, shows that fluid composition was a controlling factor for causing these differences. The Cove fault zone deformed in the presence of aqueous fluids, first a $CaCl_2$ brine and then an iron-rich fluid. The precipitation of quartz cement from the brine kept pace with brittle deformation, maintaining overall rock cohesion in the fault zone. The introduction of iron-rich fluids caused a switch from precipitation to dissolution of quartz, along with precipitation of goethite. In a damage zone along a backthrust in the Cave Mountain anticline, early deformation occurred in the presence of an aqueous fluid from which quartz was precipitated. The latest deformation, however, occurred in the presence of a methane-rich fluid, which inhibited the precipitation of quartz cement producing porous breccias and open fractures despite deformation at 6 km depth. Fluid composition not only affected cementation in the fault zones, but also the selection of grain-scale deformation mechanisms. Therefore, it is a controlling factor in determining the behavior and strength of these fault zones.

1. Introduction

The strength of a fault zone depends significantly on the mechanical and chemical effects of fluids within (Carter et al., 1990; Langseth and Moore, 1990; Scholz, 1990; Hickman et al., 1995). Mechanically, fluids reduce strength by reducing the effective normal stresses (Hubbert and Rubey, 1959; Handin et al., 1963; Secor, 1965). Fluids drive the development of secondary fractures, such as joints and faults, and assist the formation of near-surface fault rocks such as gouge and breccia (Sibson, 1977). Fluid-related chemical processes such as precipitation of cement (Chester and Logan, 1986), diffusive mass transfer (Rutter, 1983; Groshong, 1988; Knipe, 1989), hydrolytic weakening (Griggs and Blacic, 1965; Paterson, 1989; Paterson and Luan, 1990; Kronenberg, 1994; Post et al., 1996), strain-softening mineral reactions (Wintsch et al., 1995; Stewart et al., 2000; Imber et al., 2001; Holdsworth, 2004; Jefferies et al., 2006), and stress corrosion (Atkinson, 1984) can affect the strength and behavior of rocks in a fault zone, especially at higher temperatures where reaction kinetics are more favorable.

Fluid-related chemical processes are affected by fluid composition, in addition to extrinsic parameters such as temperature and pressure. For aqueous fluids, increasing ionic strength has been shown to reduce rock strength by assisting microfracture formation (Feng et al., 2001) and by lowering the free energy of fracture surfaces, and hence the shear stress needed for sliding, through adsorption of chemical species (Dunning et al., 1994; Tullis, 1994). Ionic strength also affects the solubility of many minerals, and therefore, the processes of solution and precipitation. In the case of quartz, solubility is increased with increasing ionic strength (Marshall and Chen, 1982; Fournier, 1985; Brantley et al., 1990; Dove and Crerar, 1990; Bennett, 1991; Azaroual et al., 1997a, b). Whether a fault zone weakens by pressure solution creep (Elliott, 1976) or strengthens by cementation will be affected by the composition of aqueous fluids.

Non-aqueous fluids can also significantly affect the strength of a fault zone. For example, CO_2 increases quartz strength by promoting brittle behavior at temperatures where a more ductile

* Corresponding author.
E-mail address: conasch@bgsu.edu (C.M. Onasch).

0191-8141/$ – see front matter © 2008 Elsevier Ltd. All rights reserved.
doi:10.1016/j.jsg.2008.10.010

response would be expected (Selverstone et al., 2003; Selverstone, 2005). Hydrocarbons are suspected of inhibiting the precipitation of quartz in pores and fractures (Houseknecht and Spötl, 1993; Worden et al., 1998; Marchand et al., 2000, 2002; Worden and Morad, 2000; Haszeldine et al., 2003), thereby preventing the strengthening of fault rocks through cementation.

In this paper, we evaluate the role of variations in aqueous and non-aqueous fluid composition on the structural history and style of two faults zones with contrasting fluid histories. A comparison of the studies by Cook et al. (2006) and O'Kane et al. (2007) shows that quartz arenite in the Cove fault in south-central Pennsylvania and in a map-scale backthrust in the core of the Cave Mountain anticline in West Virginia displays different structural histories and styles despite being deformed under similar temperature and pressure conditions. Although fluids were present in both fault zones throughout deformation, their compositions differed markedly, and are the focus of this paper.

2. Geologic setting

Both fault zones are located in the Alleghanian foreland thrust belt of the central Appalachians. The thrust belt consists of a roof sequence of middle Ordovician to Pennsylvanian, dominantly clastic rocks, overlying Cambrian to middle Ordovician carbonates in duplexes that rest on autochthonous Cambrian rocks (Perry, 1978; Hatcher et al., 1989).

The Cove fault cuts the northwest limb of the Big Cove anticline and juxtaposes Cambrian and younger rocks in the hanging wall with Devonian and Mississippian rocks in the syncline to the west (Fig. 1). Unlike most major thrusts in the region, which developed coevally with map-scale folding, the Cove fault post-dates most of the folding (R. Nickelsen, pers. comm., 2003) (Fig. 1). Fault evolution involved the detachment of several small horses from the footwall as displacement accumulated. The deformation intensity within the footwall horses increases northward from the intact northwest limb of the Big Cove anticline into horses that progress from containing well defined bedding to apparently massive quartz arenite with bedding largely unrecognizable in the northern horse.

The backthrust is one of two developed at the culmination of the map-scale Cave Mountain anticline (Fig. 2) (e.g., Wilson and Shumaker, 1992). The system has less than 30 m displacement and is interpreted to link with a larger, northwest-vergent thrust fault at depth (Cook et al., 2006). Although these faults contribute significantly to local shortening they are rare elsewhere in the surrounding map-scale folds (Dunne, 1996). The southeasternmost backthrust contains a damage zone (Fig. 2) that consists of a network of linking faults, zones of intense joints, and fault rocks including porous fault breccias (Fig. 3). Thus, the two fault systems in this study deform anticlines of similar size and order, but differ in that the Cove fault is a larger map-scale structure affecting much of the host fold geometry, whereas the unnamed backthrust is a secondary structure in the culmination of the host anticline.

The target lithology for this study is well-sorted, medium-grained, framework-supported quartz arenite in the Lower Silurian Tuscarora Sandstone. The sandstone is typically well cemented with less than 5% porosity (Sibley and Blatt, 1976; Cotter, 1983; Houseknecht, 1988), although irregular bed-scale cement distribution creates locally greater porosities (Heald and Anderegg, 1960). In the central Appalachians, the Tuscarora Sandstone experienced a maximum burial of approximately 6–7 km. Based on both conodont color alteration indices and burial depth, deformation of the Tuscarora Sandstone during the Alleghanian Orogeny took place at temperatures between 150–250 °C (Epstein et al., 1977; Harris et al., 1978; Onasch and Dunne, 1993; O'Kane et al., 2007; Evans pers. comm., 2006). In the Big Cove anticline, approximately 100 m of the sandstone is exposed continuously on both limbs and in the hinge. In the horses, the preserved thickness ranges between only 15 and 30 m (Fig. 1). In the Cave Mountain anticline, the Tuscarora Sandstone reaches 100 m in thickness, but the study site has a stratigraphic thickness of about 75 m (Fig. 2).

3. Nature of deformation

Deformation in the fault zones was characterized primarily from microstructures; however, mesoscale structures were also used, especially to establish a context for interpreting microstructures. In the Cove fault zone, 37 samples were collected from the intact northwest limb and at variable distances from the fault contacts of the two footwall horses (Fig. 1). In the Cave Mountain backthrust, the 21 samples were from both the damage zone and adjacent wallrock (Fig. 2). In both fault zones, sampling was done with a goal of uniform coverage within and adjacent to the zones and inclusion of the variety of rock textures and mesoscale structures. Microstructures were characterized using transmitted light and cathodoluminescence (CL) microscopy. CL was used to determine the relative abundance of cement versus detrital grains, grain-to-grain relationships, and the presence and chronology of fracture fills (Onasch, 1990; Onasch and Dunne, 1993; Laubach et al., 2004a). CL is necessary to recognize cements and fracture fills because they typically grow in optical continuity with host rock grains, making them difficult or impossible to identify with transmitted light microscopy (Sprunt and Nur, 1979; Blenkinsop and Rutter, 1986; Onasch, 1990; Laubach, 2003). Microstructural abundances were determined from point-counting 200–250 points on a rectangular grid covering the entire thin section with a nodal spacing of at least 4–5 grain diameters. For the grain at each node, all microstructures within that grain, viewed at both 25 and 100× magnification, were recorded. If no microstructures were present, "none" was recorded for that grain. From the point-count data, microstructural abundances were calculated as the percent of grains counted with a particular microstructure. Microstructural histories were determined from cross-cutting relations. Fluid histories were based on the age of cements in breccias and in fractures relative to each other and to microstructures as determined from cross-cutting relations.

3.1. Cove fault zone

The northward increase in the deformation intensity within the footwall horses is seen mesoscopically by the loss of visible bedding and the increase in the abundance of faults, breccias, and tabular bands of white cataclasite. In thin section, the increase in structural intensity is best shown by the northward increase in abundances of brittle, crystal-plastic, and pressure solution microstructures (Fig. 4). In all locations, brittle microstructures are most abundant, followed by crystal-plastic, then pressure-solution microstructures (O'Kane et al., 2007).

Some crystal-plastic deformation probably proceeded faulting because samples away from the fault zone contain undulose extinction and a few deformation lamellae. The oldest deformation associated with faulting is distributed cataclasis (Fig. 5a). Multiple, cross-cutting generations of cataclasite constitute up to 30% of the rock in the northern horse. The cataclasite consists of irregular patches of wallrock fragments in a matrix of fine-grained quartz cement that are cross-cut by all other microstructures (Fig. 6a) Deformation became more localized with the development of tabular bands of cataclasite 20 μm to 2 cm thick, discrete shear surfaces, and dilational microfractures (Fig. 6a). Overlapping in age with the microfractures are crystal-plastic microstructures, such as deformation lamellae and bands, and pressure solution structures, such as sutured grain–grain contacts. Unlike the pre-faulting crystal-plastic microstructures, which are uniformly distributed,

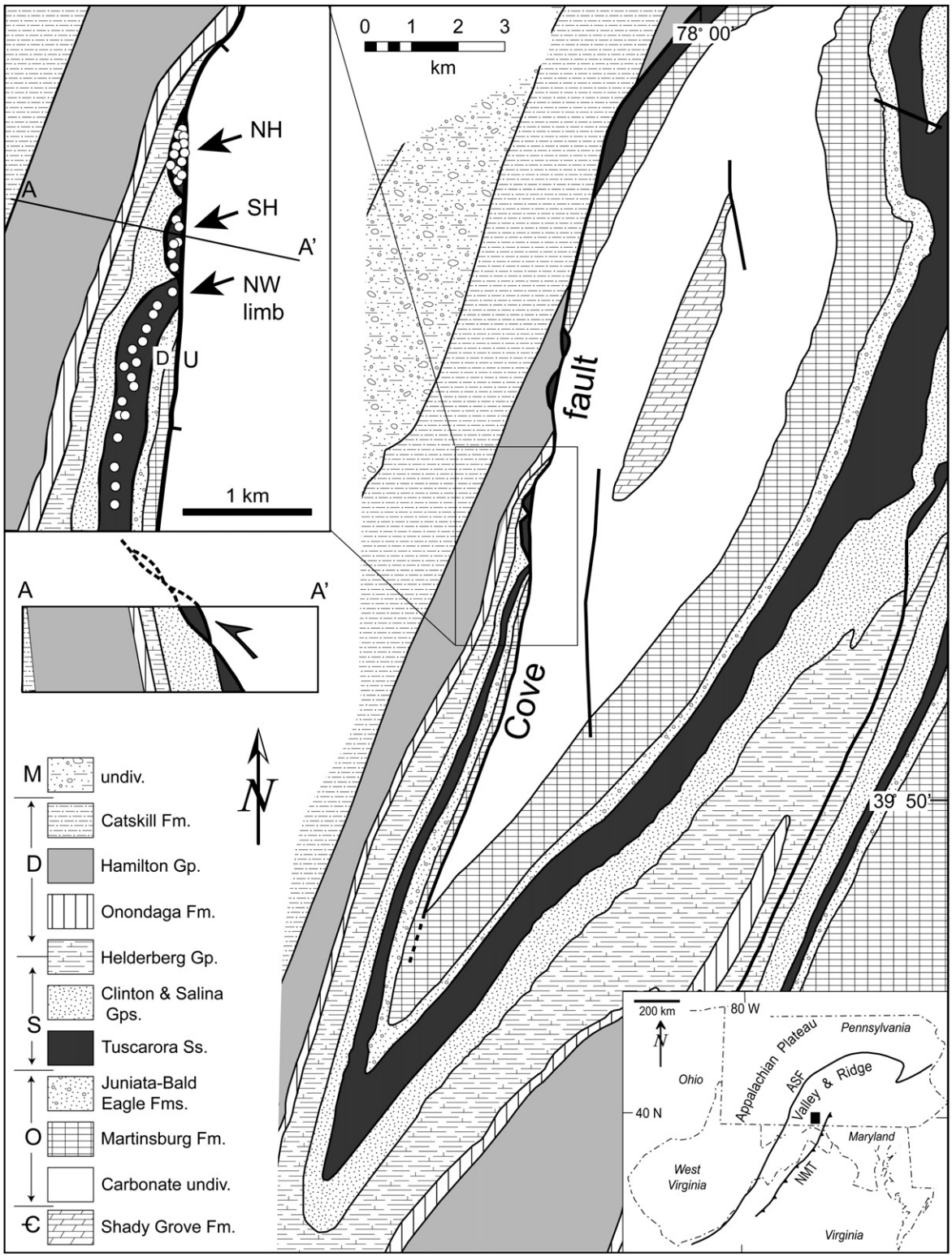

Fig. 1. Geologic map of Cove fault compiled from Geologic map of Pennsylvania (Berg et al., 1980) and unpublished mapping (Nickelsen pers. comm., 2003). Upper left inset shows detailed geology and cross section of the northwest limb of the Big Cove anticline where limb is truncated by Cove fault. North of the truncation are the southern (SH) and northern (NH) horses. Sample locations on NW limb and two horses shown with open circles. Lower right inset is the regional map showing location of the study area (solid box) and major tectonic elements in the central portion of the Appalachian foreland thrust belt. ASF – Appalachian structural front; NMT – North Mountain thrust.

microstructures of this generation tend to be localized near microfracture swarms and prominent dissolution surfaces (Fig. 6b) (O'Kane et al., 2007, Fig. 5). Whereas microfracture swarms and/or dissolution surfaces occur without the development of concentrations of crystal-plastic microstructures, the opposite was not observed. We infer that microfracture swarms and/or dissolution surfaces are a necessary precursor to the localized crystal-plastic microstructures on the basis of these spatial relationships. The youngest microstructures are fractures and large transgranular stylolites (Fig. 6c), both of which are filled with goethite.

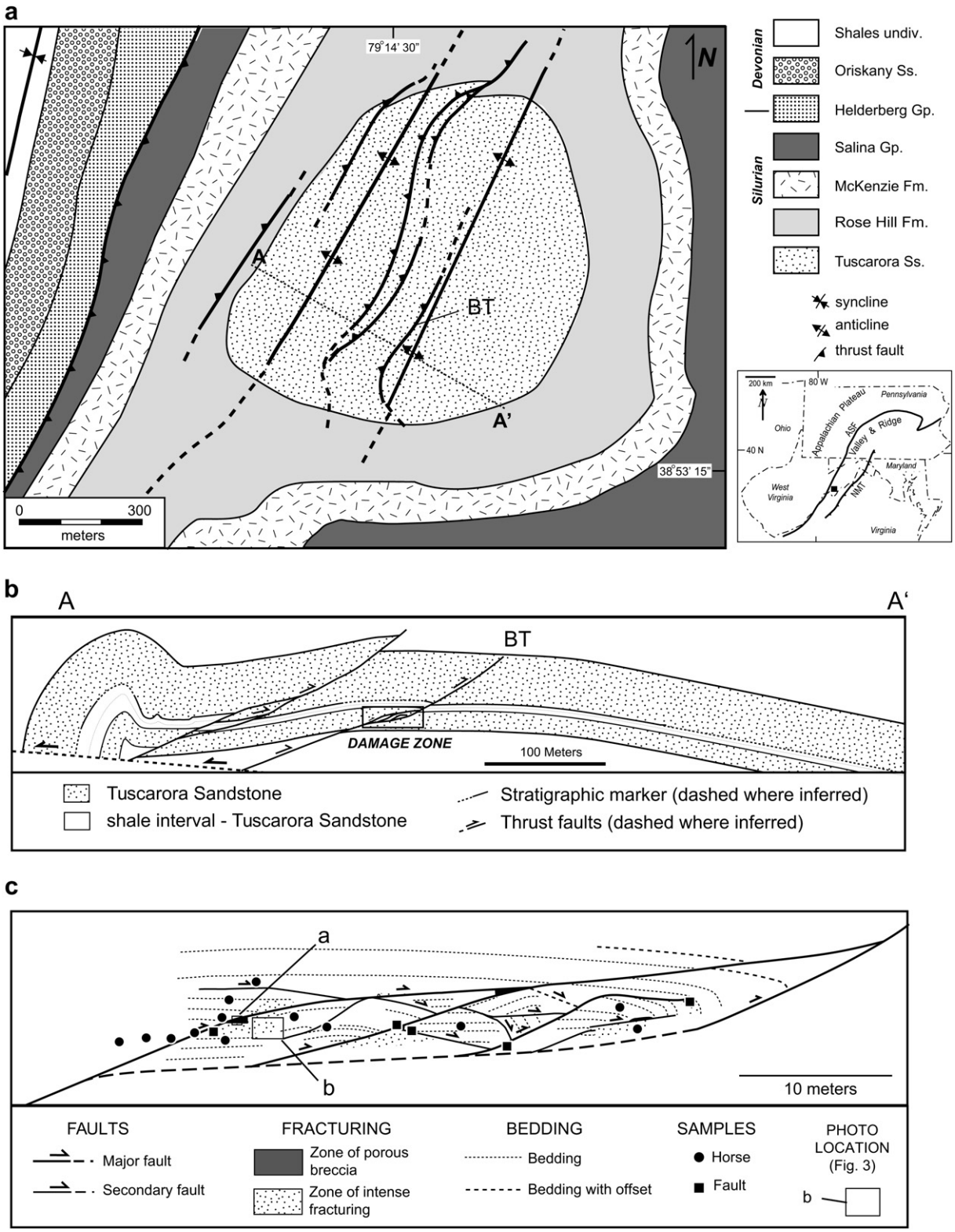

Fig. 2. Geology of the Cave Mountain backthrust area. (a) Simplified geologic map of the culmination of the Cave Mountain anticline showing the location of the backthrust damage zone in the Tuscarora Sandstone. BT – backthrust described in this study. Inset the map shows location of area in relation to regional tectonic elements. Key to features is same as in Fig. 1. (b) Cross section of the Tuscarora Sandstone along line A–A′ showing the geometry of the backthrusts and location of the damage zone. BT – backthrust described in this study. (c) Detailed cross section of the damage zone showing internal structure and location of samples used in study. Location of photos in Fig. 3 shown with boxes.

3.2. Backthrust damage zone

The backthrust is a system of faults that defines a duplex with horses (Fig. 2). It is located at an extensional step-over along the backthrust that transfers displacement from the northwest to the southeast (Cook et al., 2006). The system consists of a network of linking faults, secondary to the main backthrust, which bound zones intense jointing, smaller linking faults, and zones of fault rocks including porous fault breccias (Fig. 3). Based on the offset of bedding surfaces, the zone has accommodated $<$10 m of displacement (Cook et al., 2006).

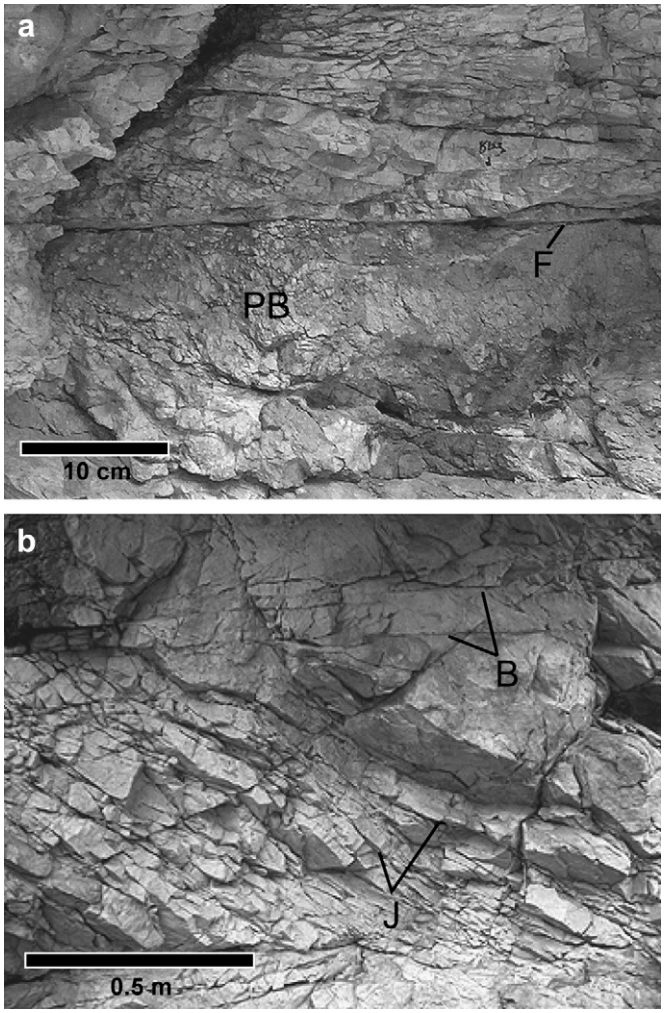

Fig. 3. Fracture characteristics within backthrust damage zone. (a) Domain of porous breccia (PB) bounded on top by subhorizontal fault (F) with downward transition from breccia to intensely fractured wallrock. (b) Intense joint (J) development within horse showing intermediate geometry between brecciated and unbreciated rock. Horizontal lines are bedding traces (B). No fractures show offset. Locations of photos (a) and (b) shown on Fig. 2c.

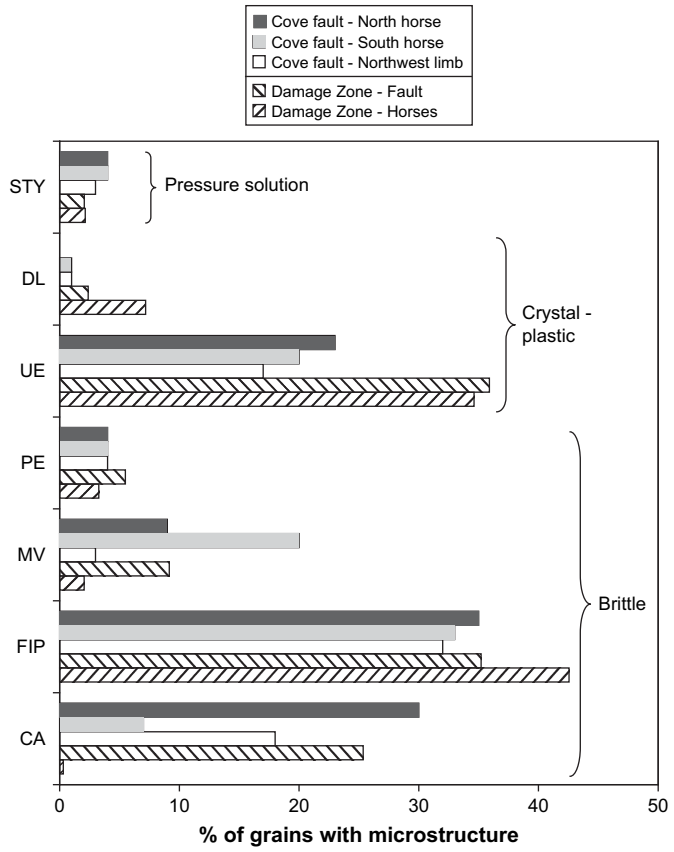

Fig. 4. Histograms of microstructural abundances in the Cove fault and backthrust damage zones. STY – transgranular and intragranular dissolutions surfaces; DL – deformation lamellae; UE – undulose extinction; PE – patchy extinction; MV – microveins; FIP – fluid inclusion planes; CA – cataclasite. Data are from microstructure point-counting of 37 thin sections in the Cove fault zone and 21 in the backthrust damage zone.

Breccias are common in the footwalls of second-order faults (Fig. 3). They are loosely consolidated in hand specimen and typically lack cement (Fig. 6d). The contact with unfractured rock is gradational and is marked by a transition to weakly brecciated rocks where clast size is large and breccia seams are narrow (Fig. 3a), and then to intensely fractured rocks where breccia is absent (Fig. 3b). On a thin section scale, overlapping shear fractures create dilational jogs with porous breccia (Fig. 6e) that mimic the geometry of the damage zone.

Microstructural abundances in the horse and fault samples of the damage zone are similar, with the exception of cataclasite, which is abundant in the fault samples, but nearly absent in horse samples (Fig. 4). When grouped by deformation mechanism, brittle microstructures are most abundant followed by crystal-plastic, then pressure solution microstructures. Abundances of individual microstructures in the damage zone are comparable to those in the Cove fault zone except for undulose extinction, which is over 50% more abundant in the damage zone than the Cove fault zone. Also, microveins in the southern horse of the Cove fault zone are more than twice as abundant as in either structural setting in the damage zone (Cook et al., 2006).

Although both the Cove fault and the backthrust are populated with similar microstructures (Fig. 4), they differ noticeably deformation history (Fig. 5). In the Cove fault zone, some crystal-plastic deformation and intergranular pressure solution may have preceded faulting, but localized crystal-plastic deformation along with extensive transgranular pressure solution occurred largely after most cataclasis (Fig. 5a). In the damage zone, crystal-plastic and pressure solution deformation occurred coevally early in the history (Fig. 5b), which is typical of regional Alleghanian deformation in the Tuscarora Sandstone (Onasch and Dunne, 1993). The onset of faulting was marked by cataclasis and related Mode I fracturing, but atypical late-stage porous breccias (Figs. 3a and 6d) and secondary release structures (Figs. 2, 3b and 6e) occurred (Cook et al., 2006). In contrast, the Cove fault zone experienced extensive late-stage dissolution and microfracturing with precipitation of goethite (Fig. 6c) (O'Kane et al., 2007), which has no correlative in the backthrust damage zone.

4. Fluids

Fluids present during deformation were characterized by the cements precipitated in fractures and voids. For quartz cement, CL microscopy and fluid inclusion microthermometry were used to characterize and further differentiate between fluids. Different generations of quartz cements were discriminated using their CL color, which is a sensitive indicator of variations in trace element chemistry (Marshall, 1988; Boggs and Krinsley, 2006). Once separated by CL color, fluid inclusion microthermometry was used to measure the temperature of homogenization (T_h), last ice melting (T_m), and eutectic (T_e) to estimate the temperature, salinity, and salt

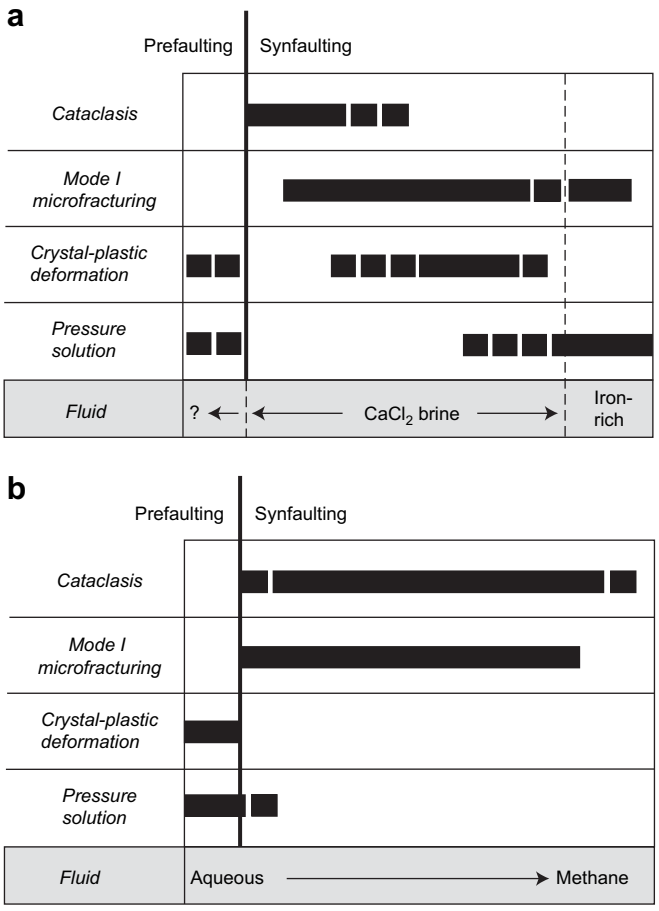

Fig. 5. Relative chronology of grain-scale deformation and fluid history for (a) Cove fault zone, and (b) backthrust damage zone.

composition, respectively, of the fluid at the time of crystal growth. All samples were also cooled to −120 °C to check for the presence of CO_2 and CH_4.

4.1. Cove fault zone

Three fluids were present during deformation in the Cove fault zone (O'Kane et al., 2007). The oldest two were $CaCl_2$-rich brines from which quartz cement was precipitated during cataclasis and dilational microfracturing (Fig. 5). Quartz precipitated from the older of the two luminesces reddish-brown (Fig. 6a) whereas the younger luminesces bluish-green. The youngest fluid, which accompanied extensive quartz dissolution in the waning stages of deformation (Fig. 5), was likely an aqueous fluid from which goethite precipitated (Fig. 6c). Both the reddish-brown and bluish-green luminescing quartz contain two-phase (L + V) aqueous inclusions (Fig. 7a). T_h data (Fig. 8a) indicate minimum trapping temperatures of 190–200 °C for the first two fluids, whereas last ice melting temperatures (T_m) that range from −11 to −24.8 °C, correspond to salinities (wt. % NaCl equivalent) of 15 to 25.9%, respectively (Fig. 8b). T_e temperatures of ~−50 °C indicate both fluids are $CaCl_2$-rich brines. Crushing experiments indicate that a few inclusions from the two oldest fluids contain a vapor phase that is soluble in kerosene, which is interpreted to be CH_4. Inclusions from the two fluids mostly overlap when plotted on a T_h versus T_m diagram (Fig. 8c) indicating that the physical conditions and salinity did not change appreciably during the first two fluid events. No temperature or salinity data were obtained for the youngest, iron-rich fluid due to a lack of fluid inclusions. The source of the iron in the youngest fluid is unknown; however, iron and manganese oxide deposits have been reported along other major faults in the central Appalachians (Monroe, 1942). Possible local sources include the iron-cemented Juniata Sandstone and iron-rich sandstones in the Rose Hill Formation that immediately underlie and overlie, respectively, the Tuscarora Sandstone.

The source of the first two fluids was investigated using oxygen isotopic compositions of the quartz cements in cataclasite and veins. Both have $\delta^{18}O$ values of ~26‰, which are markedly heavier than the wallrock ($\delta^{18}O$ ~16‰) (Table 1), implying a non-meteoric fluid source(s). Isotopically heavy fluids such as these were interpreted by Evans and Battles (1999) to have been derived from the hinterland during metamorphism and then mixed with brines and hydrocarbons during their migration to the foreland. The quartz in the Cove fault zone is 5–10‰ heavier and contains less methane than that in regional vein sets studied by Evans and Battles (1999), which are not associated with fault zones. We believe that these fluids were derived from the hinterland and were channelized in the Cove fault zone resulting in less interaction with the isotopically lighter wall rocks. (O'Kane et al., 2007).

4.2. Backthrust damage zone

Two distinctly different fluids occurred sequentially during evolution of the damage zone (Cook et al., 2006). Early microfractures and breccias were accompanied by the precipitation of quartz cement from an aqueous fluid. This fluid was trapped in two-phase aqueous (L + V) inclusions along healed microfractures, which yield a mean T_h of 168 °C. T_m data were not obtained due to the small size of the inclusions (<4 μm), so the salinity is unknown. During the later phase of deformation, cataclasis occurred with little or no quartz cementation, leaving a network of open fractures and pores in the breccias. However, abundant single-phase methane-rich inclusions (Fig. 7b) were trapped along healed microfractures in breccia clasts. T_m and T_h temperatures of the inclusions indicate that they are nearly pure methane with less than 4% CO_2 (Fig. 9). Some water must have been present because the microfractures would not heal if the fluid was pure methane; therefore, we will refer to these fluids as methane-rich. Interestingly, methane-rich inclusions are atypical of fluid trapped in inclusions of Alleghanian fractures in the Tuscarora Sandstone (e.g., Harrison and Onasch, 2000; O'Kane et al., 2007), but are common in other sandstones in the region (Evans and Battles, 1999).

The source of methane in the damage zone is believed to be the underlying Martinsburg Formation on the basis of the stratigraphic proximity of the unit and the existence of tectonic fracture networks (Cook et al., 2006). The Martinsburg is one of the four hydrocarbon source rocks identified within the Appalachian basin (Roen and Walker, 1996) and is known to contain abundant methane-rich fluid inclusions (Evans and Battles, 1999).

5. Discussion

The comparison of the fault zones in the studies by Cook et al. (2006) and O'Kane et al. (2007) shows that lithologically identical quartz arenite in the same stratigraphic unit deformed under similar physical conditions about the same time differs significantly in the deformation behavior. Rocks in both fault zones contain similar microstructures (Fig. 4); yet, striking late-stage differences in microstructural histories and textures exist (Figs. 5 and 6), which appear to be related to the differences in fluid histories between the two fault zones.

Rocks in the Cove fault zone and the backthrust were initially deformed in the presence of aqueous fluids (Fig. 5a) from which abundant quartz cement concurrently precipitated. As deformation

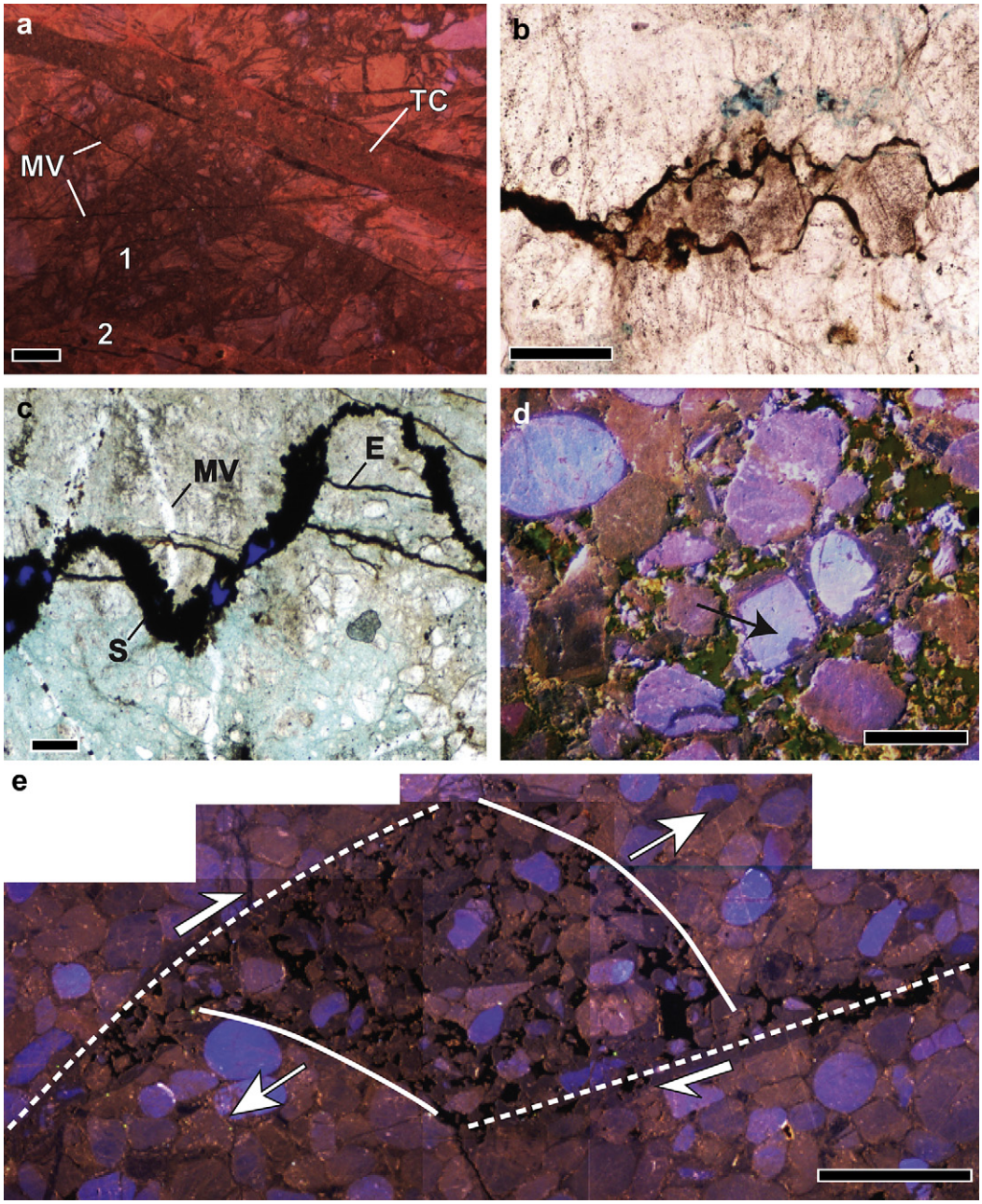

Fig. 6. Examples of microstructures from both fault zones. (a) CL image of multiple generations of cemented cataclasite (1 and 2) cut by tabular cataclasite band (TC) and microveins (MV) (Cove fault). (b) Plane light image of increased abundance of crystal-plastic microstructures near microstructures such as stylolites that were fluid pathways. Brownish grains in between two dissolution surfaces have greater occurrence of deformation lamellae and have undulose extinction with greater sweep angles than away from dissolution surfaces (Cove fault). (c) Plane light image of goethite-filled dissolution surface (S) and extension fractures (E) that truncate cataclasite and microvein (MV) (Cove fault). (d) CL image of porous breccia with clasts consisting of single grains and rock fragments. Clast indicated by arrow consists of detrital grain and partial cement rim. Olive green color is porosity filled by epoxy cement (damage zone). (e) CL mosaic of dilational jog formed by overlapping shear fractures. Note the lack of cement surrounding grain and rock fragments in jog (damage zone). Scale in each photomicrograph, except (e) is 100 μm. Scale in (e) is 1 mm.

progressed, fluids became more channelized along conduits, such as microfractures and dissolution surfaces, which have been shown to act as fluid pathways (Ortoleva et al., 1995; Dunne and Caldanaro, 1997; Smith, 2000). With access to water, hydrolytic weakening promoted crystal-plastic deformation in grains adjacent these pathways (Fig. 6b) (O'Kane et al., 2007). Later, fluids became iron-rich, causing a change from precipitation to widespread dissolution of quartz with goethite precipitation (Fig. 6c). The change in aqueous fluid composition from $CaCl_2$ brine to an iron-rich fluid greatly increased the solubility of quartz in the fluid thereby promoting extensive dissolution of quartz along fracture walls and preexisting dissolution surfaces. Whereas quartz was precipitated from the $CaCl_2$ brine during most of the deformation, goethite was precipitated in the spaces created by quartz dissolution in the waning stages of deformation. This change from the precipitation of quartz to goethite could be brought about by an increase in pH; however, the solubility of quartz is affected only by a pH above 9.0 (Fyfe et al., 1978), which, while observed in some near-surface weathering environments (Drever, 1997), is not expected of fluids in fault zones (e.g., Kerrich, 1986). Rather, redox reactions that lead to the replacement of quartz by goethite (Morris and Fletcher, 1987) are thought to be responsible (O'Kane et al., 2007).

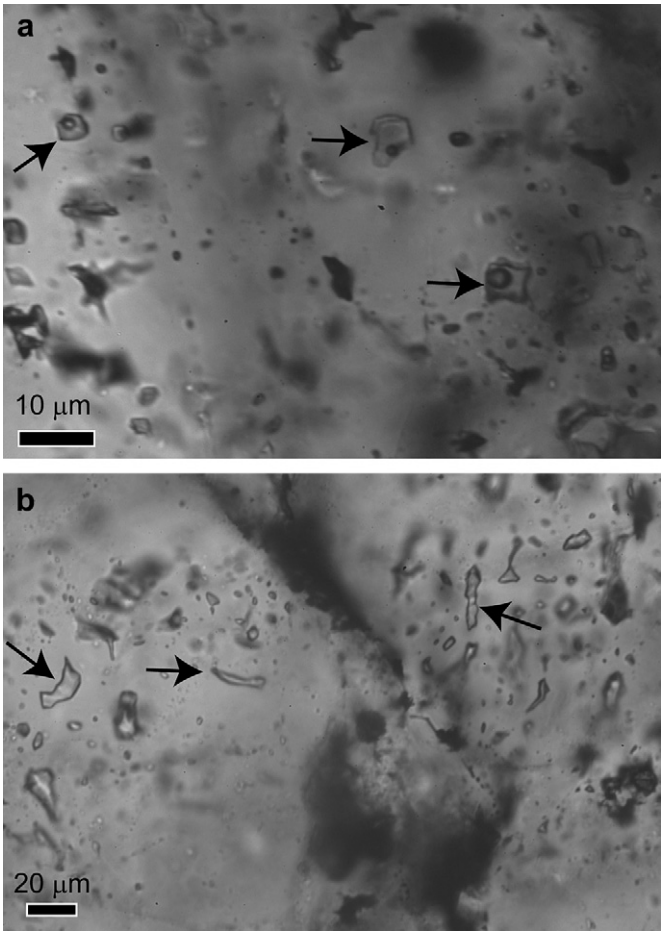

Fig. 7. Examples of fluid inclusions from the two fault zones. (a) Two-phase (L + V) aqueous inclusions in a microvein in the Cove fault zone. (b) Single-phase methane-rich inclusions in backthrust damage zone.

Prior to late-stage deformation in the backthrust damage zone, healed or sealed structures including microveins and fluid inclusion planes, as well as some breccias and cataclasite, indicate that an aqueous fluid capable of precipitating quartz was present in the damage zone (Cook et al., 2006). Either stepwise or gradually, the fluid present in the damage zone changed to dominantly methane (Figs. 5b, 7b and 9), which we interpret to have limited the precipitation of quartz cement during late-stage backthrust displacement (Fig. 6d). Because methane is chemically inert to quartz, it does not precipitate nor dissolve quartz. Although the younger fluid inclusions appeared to contain only methane, small amounts of water (up to 5%) can be present, but not detected (Shepherd et al., 1985). If so, then this water may have allowed for healing of microfractures, where surface energies are high and transport distances short. In contrast, precipitation of cement in larger pores will be controlled by the hydrocarbons that dominated the fluid.

Disagreement exists as to the effect of hydrocarbons on the precipitation of quartz cement in sandstones (e.g., Worden and Morad, 2000). A number of studies have shown that the presence of hydrocarbons impedes or prevents the precipitation of quartz cement (Worden et al., 1998; Barclay and Worden, 2000; Marchand et al., 2000, 2002; Haszeldine et al., 2003) either by wetting grain surfaces (Worden et al., 1998) or by interfering with the advective supply of silica in pore waters (Worden and Morad, 2000). Methane has been cited as the cause for the preservation of porosity in some deep gas reservoirs (Houseknecht and Spötl, 1993; Spötl et al., 1996). Other studies, however, have shown that hydrocarbons have little or no effect on quartz cementation (e.g., Walderhaug, 1990; Ramm, 1992; Aase and Walderhaug, 2005).

Some deeply buried sandstones, which have not been in contact with hydrocarbons, still preserve porosity (Laubach, 2003); therefore, factors other than the presence of hydrocarbons should be considered to explain the lack of cement in the damage zone. For example, the precipitation of quartz cement on feldspar and lithic grains is limited because they are unfavorable nucleation sites (Laubach et al., 2004a, b), but the Tuscarora Sandstone lacks these grains. Alternately, the presence of chlorite (Ehrenberg, 1993), microquartz (Aase et al., 1996; Bonnell et al., 2006), or iron oxide (Lander and Walderhaug, 1999) coatings on fracture and grain surfaces can impede or prevent quartz precipitation by reducing the substrate area available for quartz growth. Of these, only iron oxide is found in the damage zone, but it only occurs locally and not uniformly with respect to the porous breccias in the backthrust.

A decrease in the amount of pressure solution within the damage zone offers another non-methane explanation for the preservation of the secondary porosity. Renard et al. (2000) proposed that a reduction in normal stress associated with increased pore fluid pressure would lead to a reduction in the amount silica generated by pressure solution. With less silica available, cement precipitation would be reduced. This effect has been recognized in overpressured reservoirs where sandstones have less quartz cement than their normally pressured counterparts (Swarbrick, 1994; Osborne and Swarbrick, 1999; Renard et al., 2000). In the backthrust, solution-related structures are not common at any stage of deformation, so no microstructural evidence exists to indicate a change in solution rate within or adjacent to the fault zone. It appears then that unfavorable host grains, mineral coatings, or rate of pressure solution are not viable alternatives to the hypothesis that methane inhibited the precipitation of quartz cement.

The preservation of porosity in the backthrust damage zone and lack of it in the Cove fault zone could also be explained by differences in the local structural geometry. Whereas, the backthrust evolved into a release zone that favored more dilatant behavior during displacement, the geometry of the Cove fault has no such release geometry. Although dilatant zones create porosity, they also create strong fluid pressure gradients that draw fluids into opening voids (Sibson et al., 1988). Were these the same aqueous fluids present as in the early history of the damage zone, the breccias and fractures in the dilatant zone could be expected to be largely or wholly cemented. That they are not indicates to us that the fluids were not aqueous.

Given the importance of fluid chemistry on the behavior of rocks, it is also important to consider processes that may have lead to compositional differences of fluids observed in the two fault zones. Because the physical conditions in the two fault zones were similar, differences in pressure and temperature, which are important factors in controlling fluid chemistry (Fyfe et al., 1978), cannot explain the presence of different fluids. Rather, it appears that the differences are a consequence of the two faults tapping different fluid reservoirs. In the Cove fault, the oxygen isotope geochemistry of the $CaCl_2$ brines suggests that the fluids were externally derived, possibly from the metamorphic hinterland, and were channeled along regional-scale faults so as to minimize interaction with wall rocks. The backthrust, being a much smaller-scale structure, did not have access to a regional-scale fluid source and could only tap local reservoirs; such as the host Tuscarora Sandstone and later, the underlying organic-rich Martinsburg Formation.

5.1. *Importance of fluid chemistry on the behavior and strength of fault zones*

Fault strength within the frictional regime of the upper crust can be described by the Coulomb criterion (Jaeger et al., 2007), modified to account for pore fluid pressure (Hubbert and Rubey, 1959):

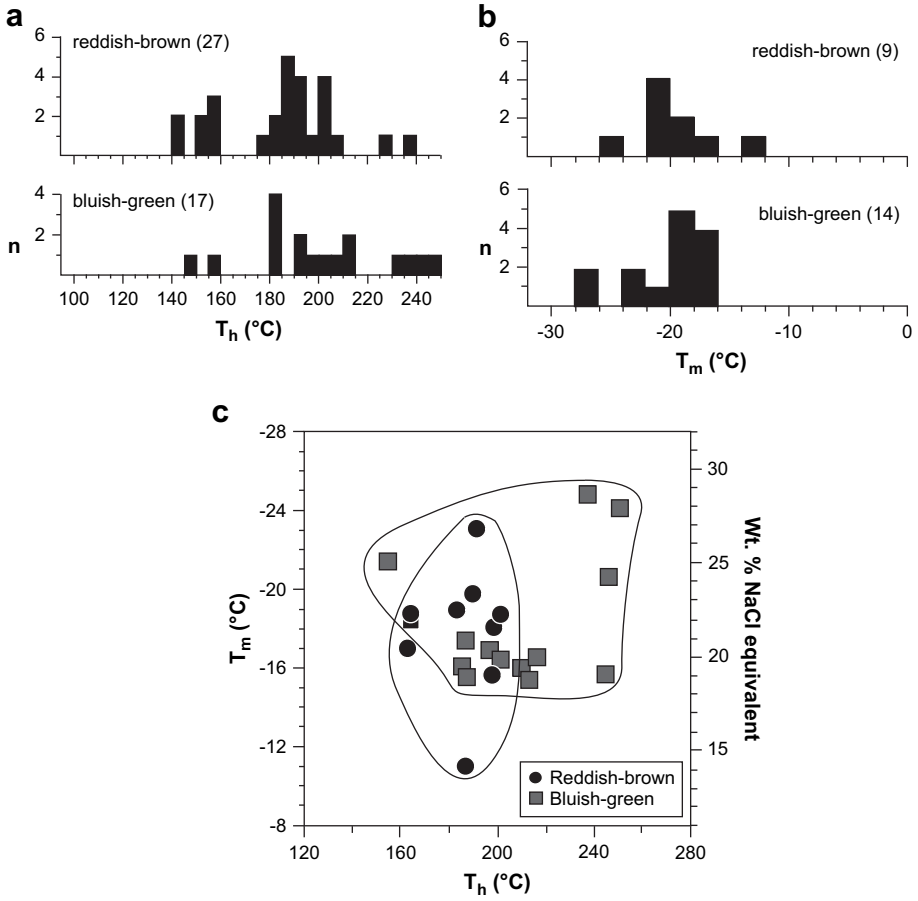

Fig. 8. Fluid inclusion data from Cove fault. Histograms of (a) homogenization (T_h) and (b) last ice melting (T_m) temperatures for two-phase aqueous inclusions from two generations of quartz cement differentiated on basis of CL color. (c) T_h/T_m plot of all inclusions where both temperatures were measured in same inclusion grouped according to cement CL color.

$$\tau = S_0 + (\sigma - p)\mu \quad (1)$$

Where t is the shear stress necessary for failure; S_0 is the cohesive strength; σ is the normal stress; p is the pore fluid pressure; and μ is the coefficient of friction. If a slip surface is present, $S_0 \approx 0$ and the fault strength is controlled by frictional behavior. Because the coefficient of friction, with the exception of clay-rich rocks, varies little between lithologies (Byerlee, 1978) the effective normal stress (σ–p) controls behavior for a pre-existing slip surface. In these circumstances fluid composition would typically not directly influence fault shear strength, because effective normal stress is controlled by the fluid pressure, which is a mechanical manifestation.

Table 1
Oxygen isotope analyses of wall rock grains and quartz precipitated in Cove fault zone.

Sample	Type	$\delta^{18}O$ (VSMOW)
CF-21	CB	26.0
CF-21 dup.	CB	26.0
CF-23	CB	23.9
CF-23 dup.	CB	24.4
CF-7	VN	26.3
CF-7	VN	25.5
CF-7 dup.	VN	26.2
CF-5	WR	14.3
CF-7	WR	15.9
CF-7 dup.	WR	15.9
CF-21	WR	16.7
CF-21 dup.	WR	16.6
CF-23	WR	15.3

CB – cataclasite band; VN – vein; WR – wallrock.

Yet, fluid composition can affect fault strength by influencing precipitation and dissolution of minerals within the fault zone, which for example, can increase cohesive strength by sealing a fault surface, alter the cohesive strength of wallrock, or change the geometry and arrangement of cataclasts affecting frictional strength. The precipitation of cement in fault rocks will increase their strength, and hence, the strength of the fault (Chester and Logan, 1986). Dissolution of minerals in the fault zone creates new pore space for fluids, which can lead to reduced strength through both mechanical effects (i.e., decreasing effective stress) or chemical effects, such as hydrolytic weakening (Kronenberg, 1994) or stress corrosion (Atkinson, 1984; Masuda, 2001). Dissolution and precipitation may be linked temporally and spatially in a source-sink relationship (Dewers and Ortoleva, 1990; Gratier et al., 2003) where fault zone strengthening from cement precipitation and weakening from pressure solution are competing processes.

During the early history of the Cove fault in the presence of an aqueous brine, strength within the fault blocks of Tuscarora Sandstone was maintained despite extensive cataclasis because precipitation of quartz cement kept pace, yielding new but rapidly-healed fractures. It is possible, although other fault zone rocks are poorly exposed, that during this time deformation and displacement shifted to rocks derived from the adjacent iron-rich Silurian Rose Hill Formation and Ordovician Juniata Sandstone because the Tuscarora Sandstone was able to maintain its strength

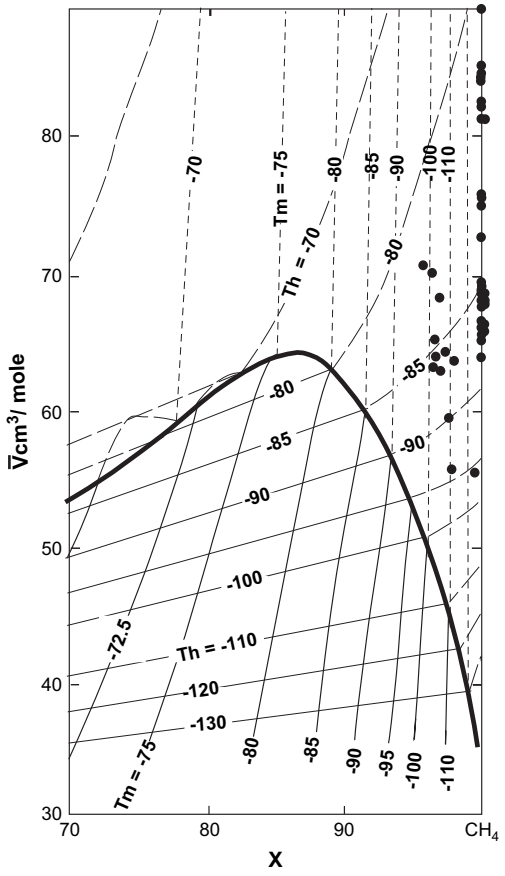

Fig. 9. Single-phase, methane-rich fluid inclusion data from backthrust damage zone. Individual inclusions (solid circles) plotted according to CO_2 solid melting (sublimation) (T_m) and hydrocarbon homogenization temperature (T_h). Most inclusions are >95% methane.

even during cataclasis. Later in the deformation, the change in fluid chemistry from a $CaCl_2$-rich brine to an iron-rich fluid favored quartz dissolution over precipitation, which likely reduced the strength of the Tuscarora fault blocks by leaving new fractures unsealed and giving fluids greater access to the fault zone. Also, these fluids aided conditions for the onset of focused crystal-plastic deformation in the vicinity of these new fluid pathways. However, these structural concentrations probably did not result in measurable displacements for the Cove Fault. Thus, the change in fluid chemistry affected the deformation behavior and internal strength of Tuscarora fault blocks, but did not at any point trigger a concentration of new displacements within the blocks, once they had formed.

During much of the propagation and displacement history of the backthrust system, an aqueous fluid was present. So, deformation in the system involved the formation of the same types of microstructures as in the Cove fault zone, but for the backthrust, these microstructures also developed in suites to accommodate all fault displacement because only quartz arenite was present. The strength of the fault zone would have fluctuated as a function of factors such as fluid pressure, cementation, and efficiency of cataclast formation (Sibson, 1977). As the methane content of the fluid became dominant during late displacement, fault strength would have changed in response to the new dilatant behavior. The change in fluid composition suppressed quartz cementation allowing new secondary pores in fault rocks and joints to form and remain open during the development of a dilatant jog, which diminished cohesion and possibly frictional strength. Thus, cataclasts were able to slide more easily and cataclastic behavior would have been favored. Overall, the fault system was weaker as compared to earlier behavior because of the relative abundance of porous fault-zone rocks and uncemented fractures in the horses. Not only would the zone be weaker without cement, but the open porosity would permit fluids to possibly accumulate and further reduce strength by increasing fluid pressure. The situation was improved for the further efficient development of a cataclastically dominant fault zone. Because this change arose at the end of the displacement history, it lead to localized formation of porous breccias at sites such as branch lines (Cook et al., 2006) rather than as a new through-going fault rock with focused displacement accumulation.

The importance of the fluid chemistry to later stage deformation in both fault zones is highlighted by considering the effects of reversing the occurrence of the fluids: methane-rich fluid in the Cove fault and aqueous fluid in the backthrust. In the former case, fractures propagating into the horses would have been uncemented, possibly allowing the horses to be comminuted and incorporated as finer fragments in the overall fault zone. In the latter case, secondary porosity may not have survived because of greater solution efficiency at cataclast point-load sites. Quite possibly, the late-stage development of different fault rocks at different geometric locations, such as a porous breccia at branch lines for active faults, would not have occurred. Instead, the character and spatial distribution of fault rocks would have been more homogeneous within the system.

6. Conclusions

A comparison of two previous studies (Cook et al., 2006; O'Kane et al., 2007) has shown that the differences in the structural style and history of quartz arenites deformed in two fault zones under similar P/T conditions are the result of differences in the fluid composition in the fault zones during deformation. In the Cove fault zone, quartz precipitation from an aqueous fluid kept pace with fracturing and cataclasis, thereby maintaining cohesion and a relatively high level of strength throughout most of the deformation. In the waning stages of deformation, a change in fluid composition from $CaCl_2$ brine to iron-rich, caused a behavior change to extensive dissolution of quartz and precipitation of goethite. In the damage zone along a backthrust in the Cave Mountain anticline, the latest stage of deformation occurred in the presence of a methane-rich fluid, which inhibited the precipitation of quartz cement leaving substantial open secondary porosity despite being deformed at depths of 6–7 km. This lack of quartz precipitation caused a significant loss in strength, not only from the lack of support provided by cement, but also from the mechanical and chemical effects associated with fluids that now had easy access to the zone.

Acknowledgements

Funding for this project was provided by the National Science Foundation (EAR-0087607), AAPG Grants-in-Aid-of-Research, Southeast GSA student research grants, and the Richard D. Hoare Research Fund at Bowling Green State University. The authors are indebted to Richard P. Nickelsen who introduced them to the Cove fault area and generously shared his unpublished data.

References

Aase, N.E., Walderhaug, O., 2005. The effect of hydrocarbons on quartz cementation: diagenesis in the Upper Jurassic sandstones of the Miller field, North Sea, revisited. Petroleum Geoscience 11, 215–223.

Aase, N.E., Bjorkum, P.A., Nadeau, P.H., 1996. The effect of grain-coating microquartz on preservation of reservoir porosity. American Association of Petroleum Geologists Bulletin 80, 1654–1673.

Atkinson, B.K., 1984. Subcritical crack growth in geological materials. Journal of Geophysical Research 89, 4077–4114.

Azaroual, M., Fouillac, C., Matray, J.M., 1997a. Solubility of silica polymorphs in electrolyte solutions, I. Activity coefficient of aqueous silica from 25° to 250 °C, Pitzer's parameterisation. Chemical Geology 140, 155–165.
Azaroual, M., Fouillac, C., Matray, J.M., 1997b. Solubility of silica polymorphs in electrolyte solutions, II. Activity of aqueous silica and solid silica polymorphs in deep solutions from sedimentary Paris basin. Chemical Geology 140, 167–179.
Barclay, S.A., Worden, R.H., 2000. Effects of reservoir wettability on quartz cementation in oil fields. In: Worden, R.H., Morad, S. (Eds.), Quartz Cementation in Sandstones. Special Publication of the International Association of Sedimentologists, vol. 29, pp. 103–117.
Bennett, P.C., 1991. Quartz dissolution in organic-rich aqueous systems. Geochimica et Cosmochimica Acta 55, 1781–1797.
Berg, T.M., Edmunds, W.E., Geyer, A.R., et al., 1980. Geologic Map of Pennsylvania. Pennsylvania Geological Survey, 4th ser., Map 1, scale 1:250,000.
Blenkinsop, T.G., Rutter, E.H., 1986. Cataclastic deformation of quartzite in the Moine thrust zone. Journal of Structural Geology 8, 669–681.
Boggs, S., Krinsley, D., 2006. Application of Cathodoluminescence Imaging to the Study of Sedimentary Rocks. Cambridge Press, Cambridge.
Bonnell, L., Larese, R.E., Lander, R.H., 2006. Porosity Preservation by Inhibition of Quartz Cementation: Microquartz Versus Hydrocarbons. AAPG Search and Discovery Article #90061.
Brantley, S.L., Evans, B., Hickman, S.H., Crerar, D.A., 1990. Healing of microcracks in quartz; implications for fluid flow. Geology 18, 136–139.
Byerlee, J.D., 1978. Friction of rocks. Pure Applied Geophysics 116, 615–626.
Carter, N.L., Kronenberg, A.K., Ross, J.V., Wiltschko, D.V., 1990. Control of fluids on deformation of rocks. In: Knipe, R.J., Rutter, E.H. (Eds.), Deformation Mechanisms, Rheology and Tectonics. Geological Society of London Special Publication, vol. 54, pp. 1–14.
Chester, F.M., Logan, J.M., 1986. Implications for mechanical properties of brittle faults from observations of the Punchbowl fault zone, California. Pure and Applied Geophysics 124, 76–106.
Cook, J., Dunne, W.M., Onasch, C.M., 2006. Development of a dilatant damage zone along a thrust relay in a low-porosity quartz arenite. Journal of Structural Geology 28, 776–792.
Cotter, E., 1983. Shelf, paralic, and fluvial environments and eustatic sea-level fluctuations in the origin of the Tuscarora Formation (Lower Silurian) of central Pennsylvania. Journal of Sedimentary Petrology 53, 25–49.
Dewers, T., Ortoleva, P., 1990. A coupled reaction/transport/mechanical model for intergranular pressure solution, stylolites, and differential compaction and cementation in clean sandstones. Geochimica et Cosmochimica Acta 54, 1609–1625.
Dove, P.M., Crerar, D.A., 1990. Kinetics of quartz dissolution in electrolyte solutions using a hydrothermal mixed flow reactor. Geochimica et Cosmochimica Acta 54, 955–969.
Drever, J.I., 1997. The Geochemistry of Natural Waters: Surface and Groundwater Environments. Prentice-Hall, New Jersey.
Dunne, W.M., 1996. The role of macroscale thrusts in the deformation of the Alleghanian roof sequence in the central Appalachians: a re-evaluation. American Journal of Science 296, 549–575.
Dunne, W.M., Caldanaro, A., 1997. Evolution of solution structures in a deformed quartz arenite: geometric changes related to permeability changes. Journal of Structural Geology 19, 663–672.
Dunning, J., Douglas, B., Miller, M., McDonald, S., 1994. The role of the chemical environment in frictional deformation: stress corrosion cracking and comminution. Pure and Applied Geophysics 143, 151–178.
Ehrenberg, S.N., 1993. Preservation of anomalously high porosity in deeply buried sandstones by grain-coating chlorite: examples from the Norwegian continental shelf. American Association of Petroleum Geologists 77, 1260–1286.
Elliott, D., 1976. The energy balance and deformation mechanisms of thrust sheets. Philosophical Transactions of the Royal Society of London. Series A 283, 289–312.
Epstein, A.G., Epstein, J.B., Harris, L.D., 1977. Conodont Color Alteration; an Index to Organic Metamorphism. U.S. Geological Survey Professional Paper, 1044–9612.
Evans, M.A., Battles, D.A., 1999. Fluid inclusion and stable isotope analyses of veins from the central Appalachian Valley and Ridge province: implications for regional synorogenic hydrologic structure and fluid migration. Geological Society of America Bulletin 111, 1841–1860.
Feng, X., Chen, S., Li, S., 2001. Effects of water chemistry on microcracking and compressive strength of granite. International Journal of Rock Mechanics & Mining Sciences 38, 557–568.
Fournier, R.O., 1985. The behavior of silica in hydrothermal solutions. In: Berger, B.R., Bethke, P.M., (Eds.), Geology and Geochemistry of Epithermal Systems. Society of Economic Geologists, Reviews in Economic Geology, no. 2, pp. 45–61.
Fyfe, W.S., Price, N.J., Thompson, A.B., 1978. Fluids in the Earth's Crust. Elsevier, Amsterdam.
Gratier, J.P., Favreau, P., Renard, F., 2003. Modeling fluid transfer along California faults when integrating pressure solution crack sealing and compaction processes. Journal of Geophysical Research 108 (B2), 28–52.
Griggs, D.T., Blacic, J.B., 1965. Quartz: anomalous weakness of synthetic crystals. Science 147, 292–295.
Groshong Jr., R.H., 1988. Low-temperature deformation mechanisms and their interpretations. Geological Society of America Bulletin 100, 1329–1360.
Handin, J., Hager Jr., R.V., Friedman, M., Feather, J.N., 1963. Experimental deformation of sedimentary rocks under confining pressure: pore pressure tests. American Association of Petroleum Geologists 47, 717–755.
Harris, A.G., Epstein, J.B., Harris, L.D., 1978. Oil and Gas Data from Paleozoic Rocks in the Appalachian Basin; Maps for Assessing Hydrocarbon Potential and Thermal Maturity (Conodont Color Alteration Isograds and Overburden Isopachs). U.S. Geological Survey Professional Paper, 0160–0753.
Harrison, M.J., Onasch, C.M., 2000. Quantitative assessment of low-temperature deformation mechanisms in a folded quartz arenite, Valley and Ridge Province, West Virginia. Tectonophysics 317, 73–91.
Haszeldine, R.S., Cavanagh, A.J., England, G.L., 2003. Effects of oil charge on illite dates and stopping quartz cement: calibration of basin models. Journal of Geochemical Exploration 78-79, 373–376.
Hatcher Jr., R.D., Thomas, W.A., Geiser, P.A., Snoke, A.W., Mosher, S., Wiltschko, D.V., 1989. Alleghanian orogen. In: Hatcher Jr., R.D., Thomas, W.A., Viele, G.W. (Eds.), The Appalachian-Ouachita Orogen in the United States. The Geology of North America F-2, pp. 233–318.
Heald, M.T., Anderegg, R.C., 1960. Differential cementation in the Tuscarora Sandstone (Virginia-West Virginia). Journal of Sedimentary Research 30, 568–577.
Hickman, S., Sibson, R., Bruhn, R., 1995. Introduction to special section: mechanical involvement of fluids in faulting. Journal of Geophysical Research 100, 12831–12840.
Holdsworth, R.E., 2004. Weak faults-rotten cores. Science 303, 181–182.
Houseknecht, D.W., 1988. Intergranular pressure solution in four quartzose sandstones. Journal of Sedimentary Petrology 58, 228–246.
Houseknecht, D.W., Spötl, C., 1993. Empirical observations regarding methane deadlines in deep basins and thrust belts. U.S. Geological Survey Professional Paper 1570, 217–231.
Hubbert, M.K., Rubey, W.W., 1959. Role of fluid pressure in mechanics of overthrust faulting. Geological Society America. Bulletin 70, 115–166.
Imber, J., Holdsworth, R.E., Butler, C.A., 2001. A reappraisal of the Sibson–Scholtz fault zone model: the nature of the frictional to viscous ("brittle-ductile") transition along a long-lived, crustal-scale fault, Outer Hebrides, Scotland. Tectonics 20, 601–624.
Jaeger, J.C., Cook, N.G.W., Zimmerman, R.W., 2007. Fundamentals of Rock Mechanics. Blackwell, Malden.
Jefferies, S.P., Holdsworth, R.E., Wibberley, C.A.J., Shimamoto, T., Spiers, C.J., Niemeijer, A.R., Lloyd, G.E., 2006. The nature and importance of phyllonite development in crustal-scale fault cores: an example from the Median Tectonic Line, Japan. Journal of Structural Geology 28, 220–235.
Kerrich, R., 1986. Fluid infiltration into fault zones: chemical, isotopic, and mechanical effects. Pure and Applied Geophysics 124, 225–268.
Knipe, R.J., 1989. Deformation mechanisms – recognition from natural tectonites. Journal of Structural Geology 1, 127–146.
Kronenberg, A.K., 1994. Hydrogen speciation and chemical weakening of quartz. In: Heaney, P.J., Prewitt, C.T., Gibbs, G.V. (Eds.), Silica, Physical Behavior, Geochemistry and Materials Applications. Mineralogical Society of America, pp. 123–176. Reviews in Mineralogy 29.
Lander, R.H., Walderhaug, O., 1999. Predicting porosity through simulating sandstone compaction and quartz cementation. American Association of Petroleum Geologists 83, 433–449.
Laubach, S.E., 2003. Practical approaches to identifying sealed and open fractures. American Association of Petroleum Geologists Bulletin 87, 561–579.
Laubach, S.E., Lander, R.H., Bonnell, L.M., Olson, J.E., Reed, R.M., 2004a. Opening histories of fractures in sandstone. In: Cosgrove, J.W., Engelder, T. (Eds.), The Initiation, Propagation, and Arrest of Joints and Other Fractures. Geological Society of London Special Publications, vol. 231, pp. 1–9.
Laubach, S.E., Reed, R.M., Olson, J.E., Lander, R.H., Bonnell, L.M., 2004b. Coevolution of crack-seal texture and fracture porosity in sedimentary rocks: cathodoluminescence observations of regional fractures. Journal of Structural Geology 26, 967–982.
Langseth, M., Moore, J.C., 1990. Introduction to special section on the role of fluids in sediment accretion, deformation, diagenesis and metamorphism in subduction zones. Journal of Geophysical Research 95, 8737–8742.
Marchand, A.M., Haszeldine, R.S., Macaulay, C., Swennen, R., Fallick, A.E., 2000. Quartz cementation inhibited by crestal oil charge: Miller deep water sandstone, UK North Sea. Clay Minerals 35, 201–210.
Marchand, A.M., Smalley, P.C., Haszeldine, R.S., Fallick, A.E., 2002. Note on the importance of hydrocarbon fill for reservoir quality prediction in sandstones. American Association of Petroleum Geologists Bulletin 86, 1561–1571.
Marshall, D.J., 1988. Cathodoluminescence of Geological Materials. Unwin Hyman, Boston.
Marshall, W.L., Chen, C.-T.A., 1982. Amorphous silica solubilities, IV. Postulated sulfate-silicic acid solution complex. Geochimica et Cosmochimica Acta 46, 367–370.
Masuda, K., 2001. Effects of water on rock strength in a brittle regime. Journal of Structural Geology 23, 1653–1657.
Monroe, W.H., 1942. Manganese deposits of Cedar Creek Valley, Frederick and Shenandoah Counties, Virginia. U.S. Geological Survey Bulletin 936-E.
Morris, R.C., Fletcher, A.B., 1987. Increased solubility of quartz following ferrous-ferric iron reactions. Nature 330, 558–561.
O'Kane, A., Onasch, C.M., Farver, J., 2007. The role of fluids in low-temperature, fault-related deformation of quartz arenite. Journal of Structural Geology 29, 819–836.
Onasch, C.M., 1990. Role of microfractures in the deformation of a quartz arenites in the central Appalachian foreland. Journal of Structural Geology 12, 883–894.
Onasch, C.M., Dunne, W.M., 1993. Variation in quartz arenite deformation mechanisms between a roof sequence and duplexes. Journal of Structural Geology 5, 465–476.
Ortoleva, P., Al-Shaieb, Z., Puckette, J., 1995. Genesis and dynamics of basin compartments and seals. American Journal of Science 295, 345–427.
Osborne, M., Swarbrick, R.E., 1999. Diagenesis of North Sea HPHT reservoirs – consequences for porosity and overpressure conditions. Marine and Petroleum Geology 16, 337–353.

Paterson, M., 1989. The interaction of water with quartz and its influence in dislocation flow-an overview. In: Karato, S. (Ed.), Rheology of Solids and of the Earth. Oxford University Press, pp. 107–142.
Paterson, M.S., Luan, F.C., 1990. Quartzite rheology under geological conditions. Geological Society Special Publications 54, 299–307.
Perry, W.J. Jr., 1978. The Wills Mountain Anticline: a Study in Complex Folding and Faulting in Eastern West Virginia. West Virginia Geological and Economic Survey Publication RI-32.
Post, A.D., Tullis, J., Yund, R.A., 1996. Effects of chemical environment on dislocation creep of quartzite. Journal of Geophysical Research 101, 22143–22155.
Ramm, M., 1992. Porosity-depth trends in reservoir sandstones: theoretical models related to Jurassic sandstones, offshore Norway. Marine and Petroleum Geology 9, 553–567.
Renard, F., Brosse, E., Sommer, F., 2000. The different processes involved in the mechanism of pressure solution in quartz-rich rocks and their interactions. In: Worden, R.H., Morad, S. (Eds.), Quartz Cementation in Sandstones. Special Publication of the International Association of Sedimentologists, vol. 29, pp. 67–78.
Roen, J.B., Walker, B.J. (Eds.), 1996. The Atlas of Major Appalachian Gas Plays. West Virginia Geological and Economic Survey Publication V-25.
Rutter, E.H., 1983. Pressure solution in nature theory and experiment. Journal of the Geological Society 140, 725–740.
Scholz, C.H., 1990. Mechanism of creep in brittle rock. Journal of Geophysical Research 73, 3295–3302.
Secor, D.T., 1965. Role of fluid pressure in jointing. American Journal of Science 263, 633–646.
Selverstone, J., 2005. Preferential embrittlement of graphitic schists during extensional unroofing in the Alps: the effect of fluid composition on rheology in low-permeability rocks. Journal of Metamorphic Geology 23, 461–470.
Selverstone, J., Holyoke, C.W., Tullis, J., 2003. Variations in quartzite rheology as a function of metamorphic fluid composition; results of coupled fluid inclusion and experimental studies. Abstracts with Programs. Geological Society of America 35, 91.
Shepherd, T.J., Rankin, A.H., Alderton, D.H.M., 1985. A Practical Guide to Fluid Inclusion Studies. Blackie, Glasgow.
Sibley, D.F., Blatt, H., 1976. Intergranular pressure solution and cementation of the Tuscarora orthoquartzite. Journal of Sedimentary Petrology 46, 881–896.
Sibson, R.H., 1977. Fault rocks and fault mechanisms. Journal of the Geological Society of London 133, 140–213.
Sibson, R.H., Robert, F., Poulsen, K.H., 1988. High angle reverse faults, fluid pressure cycling, and mesothermal gold-quartz deposits. Geology 16, 551–555.
Smith, J.V., 2000. Three-dimensional morphology and connectivity of stylolites hyperactivated during veining. Journal of Structural Geology 22, 59–64.
Spötl, C., Houseknecht, D.W., Burns, S.J., 1996. Diagenesis of an 'overmature' gas reservoir: the Spiro sand of the Arkoma Basin. USA. Marine and Petroleum Geology 13, 25–40.
Sprunt, E.S., Nur, A., 1979. Microcracking and healing in granites; new evidence from cathodoluminescence. Science 205, 495–497.
Stewart, M., Holdsworth, R.E., Strachan, R.A., 2000. Deformation processes and weakening mechanisms within the frictional-viscous transition zone of major crustal-scale faults: insights from the Great Glen Fault Zone, Scotland. Journal of Structural Geology 22, 543–560.
Swarbrick, R.E., 1994. Reservoir diagenesis and hydrocarbon migration under hydrostatic paleopressure conditions. Clay Minerals 29, 463–473.
Tullis, T., 1994. The effect of pore fluid chemistry on the friction of quartz gouge. U.S. Geological Survey Open File Report 94-228, 509–513.
Walderhaug, O., 1990. A fluid inclusion study of quartz cemented sandstones from offshore mid-Norway – possible evidence for continued quartz cementation during oil emplacement. Journal of Sedimentary Petrology 60, 203–210.
Wilson, T.H., Shumaker, R.C., 1992. Broad Top thrust sheet; an extensive blind thrust in the Central Appalachians. American Association of Petroleum Geologists Bulletin 76, 1310–1324.
Wintsch, R.P., Christoffersen, R., Kronenberg, A.K., 1995. Fluid-rock weakening of fault zones. Journal of Geophysical Research 100, 13,021–13,032.
Worden, R.H., Morad, S., 2000. Quartz cementation in oil field sandstones: a review of the key controversies. In: Worden, R.H., Morad, S. (Eds.), Quartz Cementation in Sandstones. Special Publication of the International Association of Sedimentologists, vol. 29, pp. 1–20.
Worden, R.H., Oxtoby, N.H., Smalley, P.C., 1998. Can oil emplacement prevent quartz cementation in sandstones? Petroleum Geoscience 4, 129–137.